

# Proline Behavior in Model Prebiotic Peptides Formed by Wet–Dry Cycling

Jabbari N. Ervin, Marcos Bouza, Facundo M. Fernández, and Jay G. Forsythe\*



Cite This: <https://dx.doi.org/10.1021/acsearthspacechem.0c00119>



Read Online

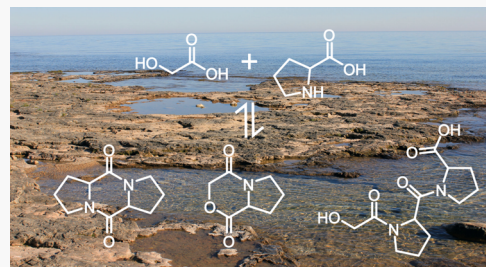
ACCESS |

Metrics & More

Article Recommendations

Supporting Information

**ABSTRACT:** The amino acid proline plays critical roles in polypeptide structure and function. However, the influence of proline residues on proto-peptide evolution is unknown. In order to begin exploring this question, we formed mixtures of model prebiotic peptides by wet–dry cycling and compared proline incorporation to that of glycine, alanine, and valine. Proline uptake was more efficient than the other amino acids into linear oligomers. However, proline was also found in small, cyclic species. In a more complex mixture of monomers and oligomers, proline displayed similar behavior—efficient uptake into linear sequences and yet also into small cyclic oligomers.



**KEYWORDS:** *origins-of-life, prebiotic chemistry, proline, depsipeptide, mass spectrometry*

## INTRODUCTION

The chemical evolution from amino acids to peptides with structure and function is of great interest to origins-of-life research.<sup>1,2</sup> Amino acid condensation is thermodynamically unfavorable in water;<sup>3</sup> hence, various approaches have been explored that make peptide bond formation feasible in model prebiotic environments.<sup>4–10</sup> Previously, we demonstrated an ester–amide exchange approach for bond formation; alpha-hydroxy acids such as glycolic acid or lactic acid condense into oligoesters and subsequently react with amino acids to form depsipeptides, copolymers of amino acids and hydroxy acids with both amide and ester linkages.<sup>11–13</sup>

Amino acids and hydroxy acids have been detected together in Miller–Urey spark discharge mixtures and meteorites<sup>14–17</sup> and react with one another under relatively mild conditions to form depsipeptides.<sup>11</sup> The barrier for amide bond formation is lowered through ester intermediates.<sup>18</sup> Depsipeptide condensation and chemical progression toward peptides occurs *via* wet–dry cycling, or heating a small aqueous pool of monomer(s) to dryness and then rehydration in a cyclical fashion.<sup>19</sup> This models warm-day/cool-night environmental processes on Earth and may occur in extraterrestrial environments such as tidal basins, hydrothermal fields, and/or deliquescent salt flats.<sup>20–25</sup>

The purpose of this study was to examine the amino acid proline (Pro; P) and compare its behavior with other amino acids in depsipeptide formation through wet–dry cycling. Pro is generally accepted as a prebiotically available monomer and is thought to be one of the earliest amino acids to be biologically encoded.<sup>26,27</sup>

Pro is not only prebiotically plausible but also rather unique amongst proteinogenic amino acids. It is the only coded residue with a secondary amine (approximately an order of

magnitude more basic than the others' primary amines<sup>28</sup>), and its peptide linkages have lower energy barriers for *cis–trans* isomerism.<sup>29</sup> Indeed, Pro *cis–trans* isomerism is often a rate-limiting step in peptide and protein folding.<sup>30–32</sup> Pro can terminate helices,<sup>33</sup> kink helices,<sup>34</sup> or form helices altogether devoid of amide hydrogens.<sup>35–38</sup>

In 2009, Pavlov et al. showed that Pro reacts slower in biological translation than the other proteinogenic amino acids yet faster than other non-proteinogenic, N-alkylated amino acids with more steric hindrance at their N-termini.<sup>39</sup> It was suggested that Pro has optimal reactivity among N-alkylated amino acids, and thus, proto-genetic codes may have selected it as the best N-substituted monomer available.

Pro exhibits interesting behavior not only in coded peptides but also as a free amino acid. It can act as an asymmetric catalyst to augment enantiomeric excesses in various reactions, including the formation of molecules relevant to prebiotic chemistry.<sup>40–45</sup> The emergence of homochirality remains an outstanding question in the field, and Pro has been studied in this context as well.<sup>46,47</sup>

We postulate that, because of its various properties, Pro may have provided distinct contributions to proto-peptide evolution. Studying the formation and composition of Pro-containing depsipeptides is the key first step in investigating this question. Specifically, we hypothesized that Pro would incorporate into depsipeptides efficiently as its secondary

Received: May 4, 2020

Revised: June 15, 2020

Accepted: July 6, 2020

Published: July 7, 2020

amine should be a good nucleophile for ester-amide exchange.<sup>48</sup> We also hypothesized that cyclic depsipeptides could emerge upon repeated wet–dry cycling, as Pro can participate in peptide turns.<sup>49</sup>

Here, we prepared depsipeptide mixtures by wet–dry cycling and compared Pro incorporation to that of three other simple and plausible amino acids: glycine (Gly; G), alanine (Ala; A), and valine (Val; V). Mass spectrometry (MS) and Fourier transform infrared (FTIR) spectroscopy were used to characterize oligomer mixtures.

## MATERIALS AND METHODS

**Materials.** Two hydroxy acids and four amino acids were monomers in this study, all from Sigma-Aldrich, USA. The hydroxy acids glycolic acid and L-lactic acid were diluted to various concentrations from 70 and 88 wt %, respectively. Gly, L-Ala, L-Val, and L-Pro were of >98% purity. Both 2,5-dihydroxybenzoic acid (DHB; >99% purity, Sigma-Aldrich USA) and sodium trifluoroacetate (Fisher Scientific) were used without additional purification. Ala–Ala diketopiperazine (99%) was obtained from Sigma-Aldrich USA, and Pro–Pro diketopiperazine was custom synthesized by Bachem. Deionized water (18.2 MΩ cm) was generated using a Thermo Barnstead MicroPure system. Optima liquid chromatography–MS (LC–MS) grade acetonitrile was obtained from Fisher Scientific, as were formic acid ampules.

**Formation of Depsipeptide Mixtures.** Monomer stock solutions were prepared at 0.40 M in deionized water. From these, 100 μL of each was combined into a new 1.5 mL Eppendorf tube to form binary mixtures of 0.20 M hydroxy acid and 0.20 M amino acid (1:1 mol ratios; 200 μL total). A more complex sample with all six monomers was made by combining stock solutions as follows: 50 μL of 0.40 M glycolic acid, 50 μL of 0.40 M lactic acid, and 25 μL of each 0.40 M amino acid. All solutions were unbuffered and acidic (pH ~ 3) because of the hydroxy acids.

Depsipeptides were formed by subjecting monomer mixtures to 1, 4, 8, or 12 wet–dry cycles. Eppendorf tubes were heated—with open caps for water evaporation—in an oven at 85 °C and 1 atm for 24 h cycles. After each cycle, samples were cooled to room temperature, rehydrated with 200 μL of deionized water, and sonicated for several seconds before reintroduction into the oven. After the final cycle, sample mixtures were stored dry at –20 °C and were then dissolved (fully) in 200 μL of 50% water/50% acetonitrile for MS experiments. FTIR samples were not rehydrated after the final drying cycle.

**MALDI-TOF MS of Binary Mixtures.** Depsipeptide mixtures with one hydroxy acid and one amino acid were analyzed on a Voyager DE-STR (JBI Scientific) matrix-assisted laser desorption/ionization–time of flight (MALDI-TOF) mass spectrometer equipped with a nitrogen gas laser (337 nm; 20 Hz). All spectra were acquired in a positive ion, reflector TOF mode. Instrument settings were as follows: +20 kV acceleration potential, 76% extraction grid, 150 ns delay, and *m/z* range of 200–2000. MALDI spots consisted of the following: 1.0 μL of solution containing 40.0 mM DHB matrix and 4.0 mM sodium trifluoroacetate (NaTFA) spotted first, followed by 0.50 μL of the depsipeptide sample solution. Plates were dried with a gentle flow of air at room temperature and pressure. Our group previously optimized this sample preparation in order to maximize depsipeptide signal and minimize matrix background.<sup>50</sup> The TOF was calibrated daily,

and it showed a typical resolving power of ~5000 *m/Δm* fwhm. TOF mass errors were less than ±0.10 Da, on average.

**Ion Trap MS and LC–MS of Binary Mixtures.** Direct infusion tandem MS (MS/MS) and quantitative LC–MS experiments were performed on a Thermo Velos Pro linear ion trap with Ultimate 3000 UPLC. Mixtures dissolved in 50% water/50% acetonitrile were diluted 1:10 with 80% water/20% acetonitrile/0.1% formic acid before direct infusion and 1:5 before LC–MS. Collision-induced dissociation (CID) tandem MS used He collision gas and 20–25 eV (lab-frame) energies. Heated electrospray ionization (ESI) source conditions were as follows: +4.0 kV spray; 250 °C capillary; 20 sheath gas (AU); 10 auxiliary gas (AU); 0 sweep gas (AU); and 50 S-lens RF level (AU). Reversed phase LC–MS experiments used a 2.1 × 150 mm Waters BEH C18 Peptide UPLC column with 1.7 μm particles and binary solvents of 98% water/2% acetonitrile/0.1% formic acid (“solvent A”) and 2% water/98% acetonitrile/0.1% formic acid (“solvent B”). The gradient was as follows: 0–2 min, ramp from 2 to 8% solvent B; 2–18 min, ramp from 8 to 30% solvent B; 18–21 min, ramp from 30 to 70% solvent B; 21–22 min, 70% solvent B; 22–23.5 min, ramp from 70 to 2% solvent B; and hold at 2% solvent B until 26 min. MS data were collected in positive ion mode for the first 21 min of the gradient, *m/z* 100–1200. An aspartic acid–glycine diketopiperazine internal standard (10.0 μg/mL) was added to all LC–MS solutions to normalize peak integrations. All injections were of 10 μL.

**UPLC-Orbitrap-MS/MS of Complex Mixtures.** An eight-cycle mixture of all six monomers (G, A, G, A, V, and P) was further diluted 1:50 with 80% water/20% acetonitrile/0.1% formic acid and was analyzed on a Thermo Orbitrap Q Exactive Plus with Vanquish UPLC system in positive ion, data-dependent acquisition (DDA) mode. An exclusion list was created from a sample blank, and MS/MS spectra were collected with a dynamic exclusion of 5 s and an AGC of 3e6. Higher-energy CID fragmentation used N<sub>2</sub> gas with 25 eV (lab-frame). Heated ESI source conditions were as follows: +3.5 kV spray; 250 °C capillary; 45 sheath gas; 10 auxiliary gas; 2 spare gas; 400 °C probe heater temp; and 50 S-lens RF. A 2.1 × 150 mm Waters BEH C18 Peptide UPLC column was used with 1.7 μm particles and a binary solvent system of water/0.1% formic acid (“solvent A”) and acetonitrile/0.1% formic acid (“solvent B”). The gradient was as follows: 0–35 min, ramp from 5 to 85% solvent B; 35–40 min, hold at 85% solvent B; 40–41 min, ramp from 85 to 5% solvent B; 41–45 min, and hold at 5% solvent B. Data were collected over the first 40 min of the gradient, and all injections were of 5 μL.

Spectral interpretation was assisted by Protein Prospector (UCSF), PEAKS,<sup>51</sup> and mMass.<sup>52</sup> In PEAKS, hydroxy acids could not be added as custom monomers, so they were treated as post-translational modifications (PTMs) of their amino acid analogues.

**FTIR and MALDI-FTICR MS of Complex Mixtures.** Attenuated total reflectance (ATR)–FTIR spectra were acquired on a PerkinElmer Frontier with Universal ATR probe (700–4000 cm<sup>–1</sup>; 2 cm<sup>–1</sup> resolution). Fourier transform ion cyclotron resonance (FTICR) MS was performed on a 12 Tesla Bruker SolariX with a MALDI ion source. A 100 Hz Smartbeam-II laser was used with power 30 (AU) and large laser focus. Other settings were as follows: 4M data points, *m/z* 70–1000, and external calibration with NaTFA. Mass resolution for FTICR experiments was ~225,000 *m/Δm* (fwhm) @ *m/z* 400. Mass errors were typically less than

$\pm 2.0$  ppm, and matrix preparation was similar to that used for TOF experiments.

## RESULTS AND DISCUSSION

**Amino Acid Monomers and Associated Nomenclature.** Two alpha-hydroxy acid monomers (glycolic acid and L-lactic acid) and four alpha-amino acid monomers with neutral side chains (Gly, L-Ala, L-Val, and L-Pro) were chosen for this study (Figure 1A). Monomers with acidic or basic side chains

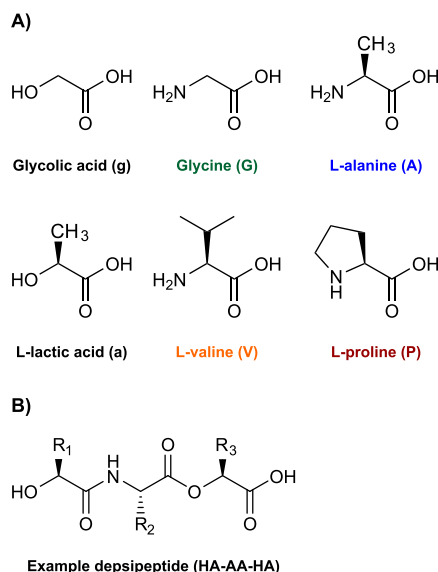


**Figure 1.** Molecules involved in this study. (A) Two hydroxy acids (g, a) and four amino acids (G, A, V, and P) were used to form depsipeptides. (B) Example of depsipeptide with terminal hydroxy acids and an internal amino acid. In addition to various depsipeptide combinations, other products in our mixtures include polyesters, peptides, with “N”-terminal hydroxy acids, and cyclic species.

were excluded as they are susceptible to isomerization, degradation, and/or branching upon heating and can complicate analysis.<sup>53–56</sup> Throughout the manuscript, hydroxy acids have been abbreviated with lower-case versions of their corresponding amino acid single-letter code (glycolic acid = g; lactic acid = a), similar to the depsipeptide nomenclature reported by Deechongkit et al.<sup>57</sup>

In order to compare Pro behavior to that of the other amino acids, solutions of one hydroxy acid and one amino acid were formed and were subjected to evaporative heating at 85 °C for repeated 24 h cycles. The major products of wet–dry cycling were depsipeptides (Figure 1B), yet unreacted monomers, pure-hydroxy acid polyesters, pure-amino acid peptides, hydroxy acid-initiated peptides, and cyclic species were also present. We refer to such solutions as “binary mixtures,” as each contained only two monomers.

**Amino Acid Incorporation in Binary Mixtures.** The formation of depsipeptides in binary mixtures after wet–dry cycling was confirmed by MALDI-TOF MS. Mass spectra of glycolic acid depsipeptides with varying amino acids (g + X) after eight cycles are provided in Figure 2. All four combinations, glycolic acid + Gly (g + G), glycolic acid + Ala (g + A), glycolic acid + Val (g + V), and glycolic acid + Pro (g + P), produced oligomers of varying composition and length. The majority of depsipeptides were detected as [M + Na]<sup>+</sup> ions because of the addition of NaTFA to the DHB

matrix. Cationization likely reduces differences in ionization efficiency between monomers, as oligomer carbonyl oxygens wrap around ions.<sup>58</sup>

For g + G, g + A, and g + V, greater than 90% of detected oligomers were linear (Figure 2A–C; MALDI Appendix, Supporting Information). Several water-loss, or [M + H – H<sub>2</sub>O]<sup>+</sup>, ions were also observed; we assigned them as short, cyclic depsipeptides that arose through intramolecular degradation (*vide infra*). Nevertheless, the vast majority of Gly, Ala, and Val depsipeptides were linear. This is unsurprising, as it is unlikely for the termini of longer chains to find one other for cyclization.<sup>59</sup>

In contrast, g + P mass spectra contained many [M + H – H<sub>2</sub>O – CO]<sup>+</sup> ions (Figure 2D; MALDI Appendix, Supporting Information). These ions were particularly intense with higher ratios of Pro to glycolic acid and likely resulted from uncontrolled in-source decay (ISD) fragmentation in the MALDI source. The matrix used in these experiments, DHB, is known to induce ISD<sup>60</sup> and particularly so with low matrix-to-analyte ratios. [M + H – H<sub>2</sub>O – CO]<sup>+</sup> ions were not observed when g + P was analyzed by electrospray ionization (ESI) - MS (Figure S1, Supporting Information), suggesting these ions did arise *via* ISD of linear oligomers. In-source fragments tentatively identified as [M + H – H<sub>2</sub>O – CH<sub>2</sub>]<sup>+</sup> were observed a + P spectra in addition to the [M + H – H<sub>2</sub>O – CO]<sup>+</sup> fragments for g + P (MALDI Appendix, Supporting Information).

All glycolic acid (g + X) oligomers and lactic acid (a + X) oligomers identified in MALDI-TOF spectra are listed in the MALDI Appendix (Supporting Information); their composition and oligomer lengths as a function of wet–dry cycling are summarized in Figure 3.

Amino acid content for each oligomer was determined by dividing the number of amino acids by its total number of amino acids and hydroxy acids, as shown in eq 1 below.

$$\frac{\#AA}{\#AA + \#HA} \quad (1)$$

The composition of individual oligomers ranged from pure polyester (0% amino acid) to depsipeptide (0% < amino acid <100%) and even pure peptide (100% amino acid). Various combinations were resolved by TOF MS, even when hydroxy acids and amino acids were separated in mass by 0.98 Da (g + G and a + A).

Amino acid content was averaged for all oligomers in each mixture (Figure 3A,B, top panels), and uptake efficiency into depsipeptides was compared. Of the four amino acids, Pro had the highest uptake efficiency, followed by Gly, Ala, and then Val (Figure 3A,B, top panels). We attribute high Pro incorporation to its secondary amine, which is more nucleophilic than the primary amines of Gly, Ala, and Val. Notable examples of Pro oligomers with high amino acid content in the mass spectrum (Figure 2D) include 4P (100% amino acid), 1g + 6P (86% amino acid), and 2g + 8P (80% amino acid). For all combinations, amino acid content increased with wet–dry cycling, consistent with prior work.<sup>11</sup>

It is important to distinguish average amino acid content from absolute abundances of species. Because of the complexity of mixtures and a lack of available standards, it was not feasible to do absolute quantitation of depsipeptides. Quantitative analysis on a similar system has been done previously, yet the lack of standards required a forced hydrolysis step in which all ester bonds in depsipeptides

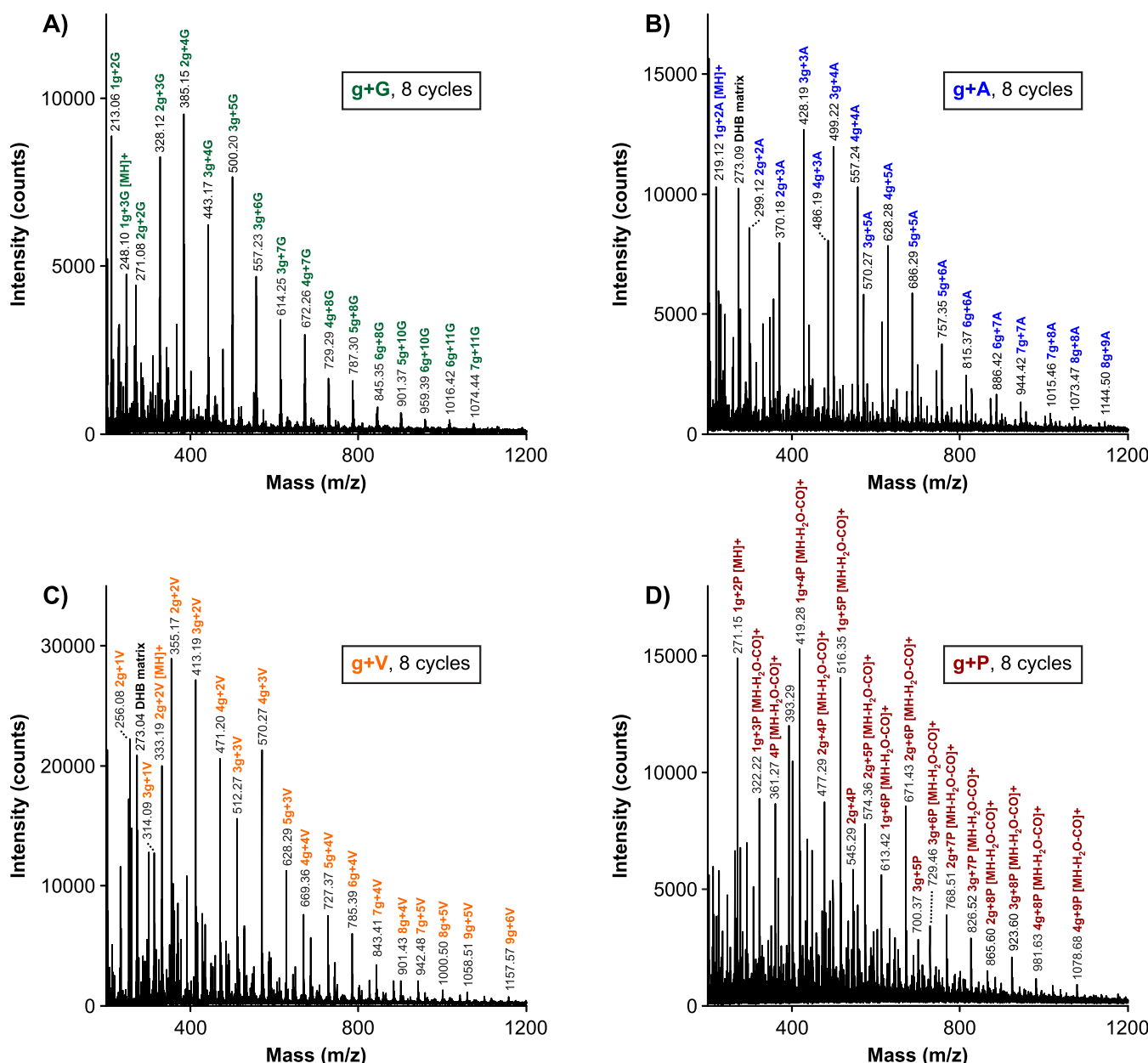


**Figure 2.** MALDI-TOF mass spectra of glycolic acid and amino acid binary mixtures after eight wet–dry cycles. Labeled depsipeptide ions are  $[M + Na]^+$  unless otherwise noted, as NaTFA was added to the DHB matrix to improve ion yields and simplify spectral interpretation. For Gly, Ala, and Val, nearly all depsipeptides were linear. However, intense  $[M + H - H_2O - CO]^+$  ions were observed for depsipeptides with high Pro content (panel D). All spectra were collected with an  $m/z$  range of 200–2000, but  $m/z$  200–1200 are shown for clarity.

were broken and only pure-peptide sequences remained.<sup>13</sup> In this study, we sought to focus on intact depsipeptides.

Uptake trends for Gly, Ala, and Val can be rationalized by solubility and (lack of) steric hindrance from the side chain. During wet–dry cycling, not all of the products were fully soluble in water. Yu et al. previously showed that hydrophobic monomers and their oligomers can precipitate during wet–dry cycling.<sup>12</sup> Ideally, to form depsipeptides, water activity should be low but not too low—if species are not exposed to any solvent, then they cannot undergo ester hydrolysis. Ester hydrolysis, in turn, produces depsipeptides with higher relative content of amino acids. This would explain why we observed low amino acid content in Val depsipeptides (in particular, a + V, as lactic acid is also more hydrophobic than glycolic acid). Moreover, as side chain bulk increases (Val > Ala > Gly; see

Figure 1A), monomers become more sterically hindered, which may have reduced the overall efficiency of ester-amide exchange. We note that although Pro had higher incorporation efficiencies in depsipeptides than Gly, Ala, and Val, analysis of Murchison suggests that Pro may have been present at lower concentrations in prebiotic environments.<sup>61</sup>

For all mixtures, oligomer lengths were the greatest between four and eight cycles (Figure 3A,B, bottom panels). The longest depsipeptide observed in these experiments had 19 residues (17a + 2V; MALDI Appendix, Supporting Information), and the longest depsipeptides with >50% amino acid content had 18 residues (7g + 11G and 8g + 10G; MALDI Appendix, Supporting Information). In a previous manuscript, we detected a depsipeptide with 21 residues.<sup>50</sup> After 12 cycles, elongation was stunted, likely due to monomer consumption.

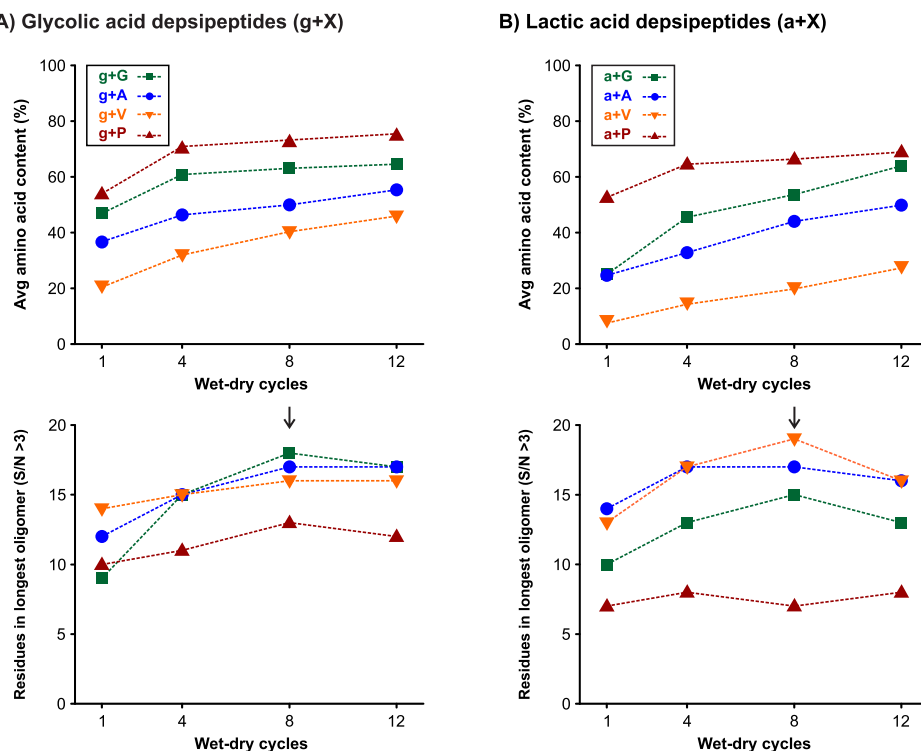


**Figure 3.** Summary of MALDI-TOF MS data for (A) glycolic acid, or  $g + X$ , depsipeptides and (B) lactic acid, or  $a + X$ , depsipeptides. Depsipeptides with Pro had the highest relative amino acid incorporation, yet the shortest lengths. For the other three experimental mixtures, lower solubility and/or more steric hindrance resulted in less amino acid incorporation (Val < Ala < Gly). Oligomer lengths leveled off after eight cycles because of monomer consumption and/or evaporation, as noted with arrows.

Continued seeding of amino acids during cycling can extend chains,<sup>13,62</sup> but this was not the emphasis of our study. Additionally, glycolic acid and lactic acid are prone to evaporation during the dry phase and can leave the open system.<sup>13</sup> In prebiotic environments, it is possible that monomers could have been recycled through rain, tides, or other processes; yet, for simplicity, we added hydroxy acid and amino acid monomers at the first cycle only.

Interestingly, for both glycolic acid- and lactic acid-depsipeptides, Pro species were shorter than those with Gly, Ala, or Val (Figure 3A,B, bottom panels). Depsipeptides with high amino acid content are generally shorter when ester-amide exchange is favored over ester elongation. However, another potential explanation is Pro sequestration in small, cyclic byproducts such as diketopiperazines (DKPs). Recent studies have shown DKP formation in model prebiotic reactions using base and trimetaphosphate.<sup>63,64</sup> Our reactions occurred at pH  $\sim 3$ , but cyclization processes can be acid- or base-catalyzed.<sup>65</sup>

**Comparison of Alanine and Proline Cyclization.** In order to investigate cyclization, we carried out experiments to compare and contrast Ala and Pro behavior in their respective binary mixtures. Two limitations of our MALDI-TOF MS method were inability to resolve sequence isomers with the same monomers (e.g., gAAg vs gAgA) and reduced spectral quality below  $m/z$  200 due to matrix interference. Small cyclic molecules of interest have masses lower than 200 Da; so, ESI techniques (LC-ESI-MS and ESI-MS/MS) were employed instead.

LC-MS standard curves for Ala-Ala DKP (Figure 4A) and Pro-Pro DKP (Figure 4B) were generated and amino acid sequestration in DKP was quantified in  $g + A$  and  $g + P$

mixtures (Figure 4C; Tables S1 and S2, Supporting Information). In both sets of mixtures, amino acid sequestration in DKP was low, less than 3% across eight cycles. This contrasts with many peptide condensation approaches for which DKP is a major product.<sup>66</sup> Nevertheless, we observed higher amounts of Pro-Pro DKP in  $g + P$  mixtures than Ala-Ala DKP in  $g + A$  mixtures after eight cycles (Figure 4C). Sequestration of Pro in its DKP form could have partially accounted for the reduced lengths of its linear depsipeptides, yet it was not a major roadblock.

Direct-infusion ion trap ESI-MS/MS was also performed to compare sequences of short linear depsipeptides (Figure 5). Spectra for the linear dimers of Ala and Pro—1g + 1A (Figure 5A) and 1g + 1P (Figure 5B)—both show amino acids on the C-termini and glycolic acid on the “N”-termini (gA and gP, respectively). However, neutral losses from each parent ion were quite different. For gA, the base peak of the fragment spectrum was the  $\text{CO}_2$  loss. For gP, the base peak was loss of  $\text{H}_2\text{O}$  and CO ( $m/z$  128), similar to the  $[\text{M} + \text{H} - \text{H}_2\text{O} - \text{CO}]^+$  ions observed in  $g + P$  MALDI spectra (Figure 2D). The high relative intensity of this ion reflects its gas-phase stability. Hayakawa et al. previously subjected Gly-Pro (GP) and Pro-Gly (PG) dipeptides to MS/MS, and GP produced a significant  $[\text{M} + \text{H} - \text{H}_2\text{O} - \text{CO}]^+$  fragment ion, whereas PG did not.<sup>67</sup> This provides additional support for such ions as products of uncontrolled MALDI ISD fragmentation in Figure 2D and particularly when Pro residues are on the C-terminus.

For linear trimers—1g + 2A (Figure 5C) and 1g + 2P (Figure 5D)—each MS/MS spectrum contained two sets of  $y_2$  fragment ions. Therefore, two sequence isomers were present in each; ones with glycolic acids on the “N”-termini, gAA and gPP, and ones with internal glycolic acids, AgA and PgP.

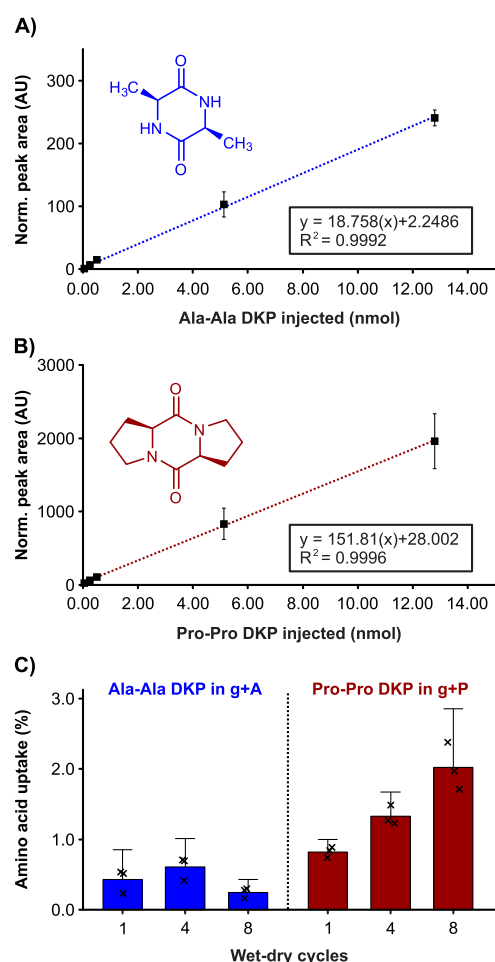


**Figure 4.** DKP formation is low during wet–dry cycling but more substantial for Pro than for Ala. (A) Ion trap LC–MS standard curve for Ala–Ala DKP, run in triplicate with error bars representing one SD. (B) LC–MS standard curve for Pro–Pro DKP, run in triplicate with error bars representing one SD. (C) Pro–Pro DKP slowly accumulated in g + P mixtures, whereas Ala–Ala DKP did not accumulate in g + A mixtures. Each sample was analyzed in triplicate, and error bars represent 95% confidence intervals.

Typically, depsipeptides formed by wet–dry cycling contain an “N”-terminal hydroxy acid as a consequence of ester-amide exchange. Observation of sequences with N-terminal amino acids (AgA and PgP) suggests either C-terminal esterification of amino acids or intramolecular cyclization of longer chains to morpholinedione followed by hydrolysis. We suppose the former would occur more for Ala and the latter for Pro (Scheme 1), which can populate a greater relative proportion of *cis* conformations. Recent studies have shown a propensity for N-terminal peptide truncation and DKP formation with *cis*-Pro at the second position.<sup>68,69</sup> Therefore, it is reasonable to conclude that *cis*-Pro conformations did induce cyclization in our mixtures, albeit to a minor degree. It should be noted that the relative abundances of both sets of  $y_2$  ions in Figure 5C,D reflect gas-phase ion stabilities and not solution-phase populations of hydroxy acids *versus* amino acids at N-termini.

Intramolecular cyclization was not exclusive to Pro, however. Several MALDI ions in non-Pro mixtures were assigned as cyclic depsipeptides [*e.g.*, cyclo(1a + 2A) and cyclo(2a + 2A) in a + A mixtures; Table S27, MALDI Appendix, Supporting Information], and as shown in Figure 4C, Ala–Ala DKP was

present in g + A mixtures. We do not suggest that Pro is required for cyclization. Instead, just as Pro–Pro DKP accumulated more than Ala–Ala DKP, we speculate that Pro-containing morpholinediones and cyclic oligomers accumulate more than those without Pro. It remains that the majority of products, with or without Pro, were linear under the conditions tested (85 °C heating, 24 h cycles, pH ~ 3).

**Proline Behavior in a More Complex Mixture.** All six monomers (g, a, G, A, V, and P) were combined and subjected to eight wet–dry cycles in order to determine if the above Pro behavior translated to a more complex and prebiotically-plausible mixture. ATR-FTIR analysis of this sample confirmed that depsipeptides were the major products, as intense ester ( $1740\text{ cm}^{-1}$ ), amide I ( $1646\text{ cm}^{-1}$ ), and amide II ( $1533\text{ cm}^{-1}$ ) bands were observed (Figure 6A). Because of the limited peak capacity and mass accuracy of the MALDI-TOF instrument, we used a high-resolution, accurate-mass Orbitrap mass spectrometer to characterize the sample in more detail. Reversed-phase UPLC-MS/MS analysis was carried out in DDA, positive-ion mode.

Consistent with the results from the binary mixtures, the vast majority of oligomers detected in the complex mixture were linear depsipeptides. The base peak chromatogram is shown in Figure 6B; 2329 spectral features ( $m/z$ , retention time, MS/MS fragments) were tentatively matched to linear g, a, G, A, V, or P oligomers with high mass accuracy ( $\pm 3$  ppm or less). In order to provide an estimate of the error associated with our matching approach, we repeated the matching process looking only for amino acids not present in our mixtures (Asp, D; Leu, L; Lys, K; and Trp, W). When doing so, 311 spectral features were matched to  $\pm 3$  ppm or less; this suggests an overall error rate of  $\sim 13\%$  (311/2329). The *de novo* software package used could not directly encode hydroxy acids as custom monomers, so we treated them as modified amino acids. Yet, there are inherent differences between hydroxy acid and amino acid fragmentation, and these likely contributed to the relatively high error rate. Therefore, all sequences of interest in this manuscript were manually validated. Selected examples of extracted ion chromatograms (XICs) and MS/MS spectra of linear oligomers are provided in Supporting Information (Figures S2–S6). N-terminal amino acids were observed in linear depsipeptides at times (*e.g.*, Figure S4, Supporting Information), consistent with prior findings for binary mixtures (Figure 5 and Scheme 1). The full UPLC-Orbitrap DDA data set is available as an open-source mzML file upon request.

Both morpholinediones and DKPs, with and without Pro, were in the complex mixture. XICs for the gP morpholinedione and Pro–Pro DKP are provided in Figure 6C,D, respectively. Both were detected with high mass accuracy, and their MS/MS spectra contained diagnostic Pro immonium ions at  $m/z$  70.0658. Examples of other cyclic dimers with Pro include lactic acid-Pro (aP) morpholinedione, Gly–Pro (GP) DKP, and Val–Pro (VP) DKP (Figures S7–S9, Supporting Information). Examples of cyclic dimers without Pro include glycolic acid-Val (gV) morpholinedione, Ala–Val (AV) DKP, and Val–Val (VV) DKP (Figures S10–S12, Supporting Information). No morpholinediones or DKPs were detected without either Pro or Val, yet these would have been below the  $m/z$  150 cutoff for MS<sup>1</sup> in our method. Therefore, MALDI-FTICR MS was used to look for small cyclics in this mixture also, with a low  $m/z$  cutoff of 70 (Figure S13, Supporting Information). Only five cyclic dimers were detected, but again, all contained Pro or Val (Table S3, Supporting Information).

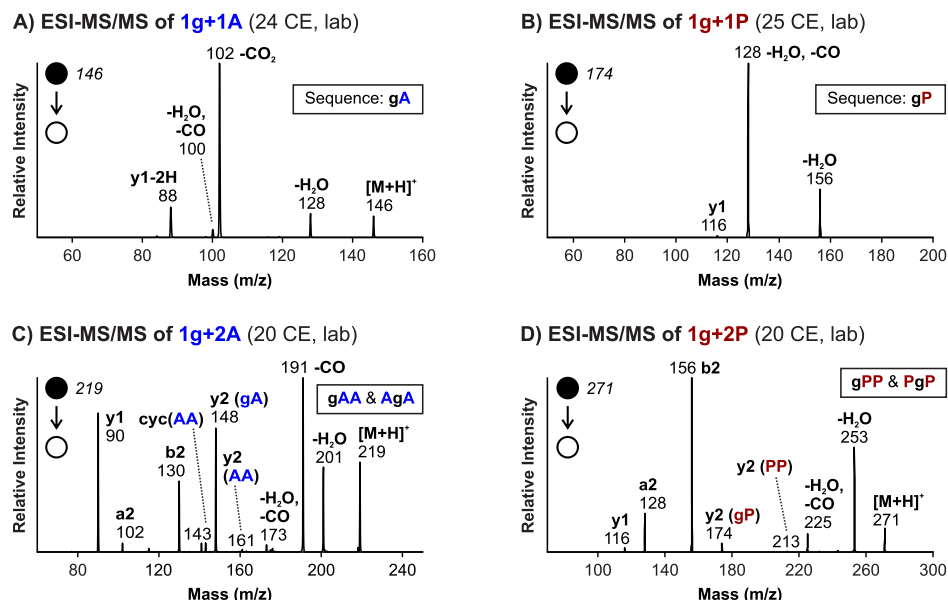
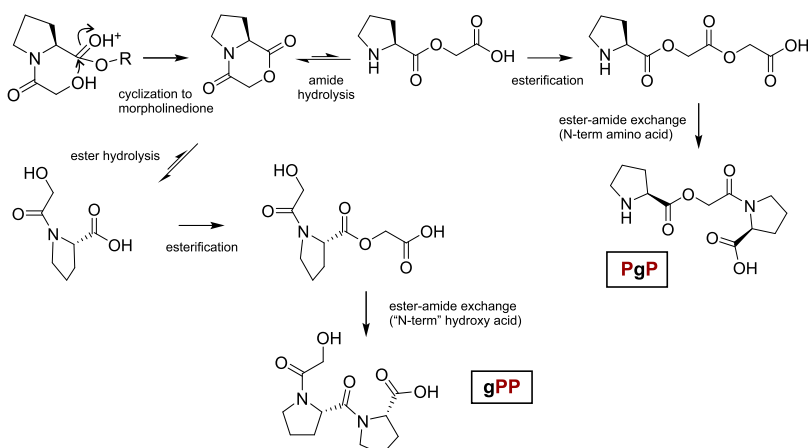


**Figure 5.** Direct infusion ESI-MS/MS sequencing of short, linear depsipeptides on an ion trap reveals N-terminal scrambling; however, such behavior is not exclusive to Pro. ESI-MS/MS spectra for (A) 1g + 1A, (B) 1g + 1P, (C) 1g + 2A, and (D) 1g + 2P depsipeptides are shown with CID collision energies ranging between 20–25 eV (“lab-frame,” or unadjusted for center-of-mass). Linear dimers are both initiated with a hydroxy acid, but both sets of trimers show N-terminal sequence scrambling (AgA and PgP).

**Scheme 1. Proposed Pathway for N-Terminal Sequence Scrambling of 1g + 2P Trimer<sup>a</sup>**



<sup>a</sup>Acid-catalyzed carbonyl protonation, cyclization *via* *cis*-Pro, and ester cleavage produces a morpholinedione, which can then be reversibly hydrolyzed back to the linear species. Ester hydrolysis is favored over amide hydrolysis, yet both occur to some degree at 85 °C and pH ~ 3. Elongation *via* esterification and ester-amide exchange leads to sequences with both glycolic acid and Pro on the “N”-terminus.

In a relevant 2014 study, Parker et al. reanalyzed Stanley Miller’s 1958 cyanamide spark discharge mixture—much more complex than ours here—and also observed cyclic dimers such as Gly–Pro DKP.<sup>70</sup> Although there are entropic costs to cyclization (perhaps less so with Pro<sup>71–73</sup>), such processes occur not only in simple mixtures but also in complex ones.

Additionally, cyclic oligomers with  $n \geq 3$  residues were detected. The XIC and MS/MS spectrum for the linear depsipeptide 1g + 1G + 1V + 1P are shown in Figure 6E; we assigned it as gPGV with 100% sequence coverage. Its cyclic analogue, cyclo(1g + 1G + 1V + 1P), is shown in Figure 6F. As in MALDI-TOF MS, it can be difficult to differentiate cyclic oligomers from in-source, water-loss fragments of linear oligomers. However, these can be resolved by UPLC. The cyclic depsipeptide eluted from the column at 13.91 min, much later than its linear counterpart (6.86 min). The water-loss

signal from the linear depsipeptide was also detected at 6.85 min (Figure 6F), providing further distinction of the two.

Sequencing cyclo(1g + 1P + 1G + 1V) was more challenging than its linear depsipeptide, however. Cyclic oligomers lack termini and can reorder in the gas phase.<sup>74</sup> An additional complication is sequences with Pro are susceptible to gas-phase scrambling.<sup>75</sup> Nevertheless, we tentatively assigned it as cyclo(gPGV) based on several factors. First, the  $b_2 + CO$  ion ( $m/z$  185.0925) not only confirmed its cyclic nature— $b + CO$  fragments are frequently observed for cyclic peptides and depsipeptides<sup>76</sup>—but also suggested connectivity. This ion,  $b_2 + CO$  [2|3, 1–2] according to the nomenclature of Niedermeyer and Strohalm<sup>52</sup> was formed by gas-phase cleavage between the second and third residues and donation of the gP CO moiety to GV (*i.e.* neutral-loss of the gP “a” fragment). Second, the abundance of neutral losses containing

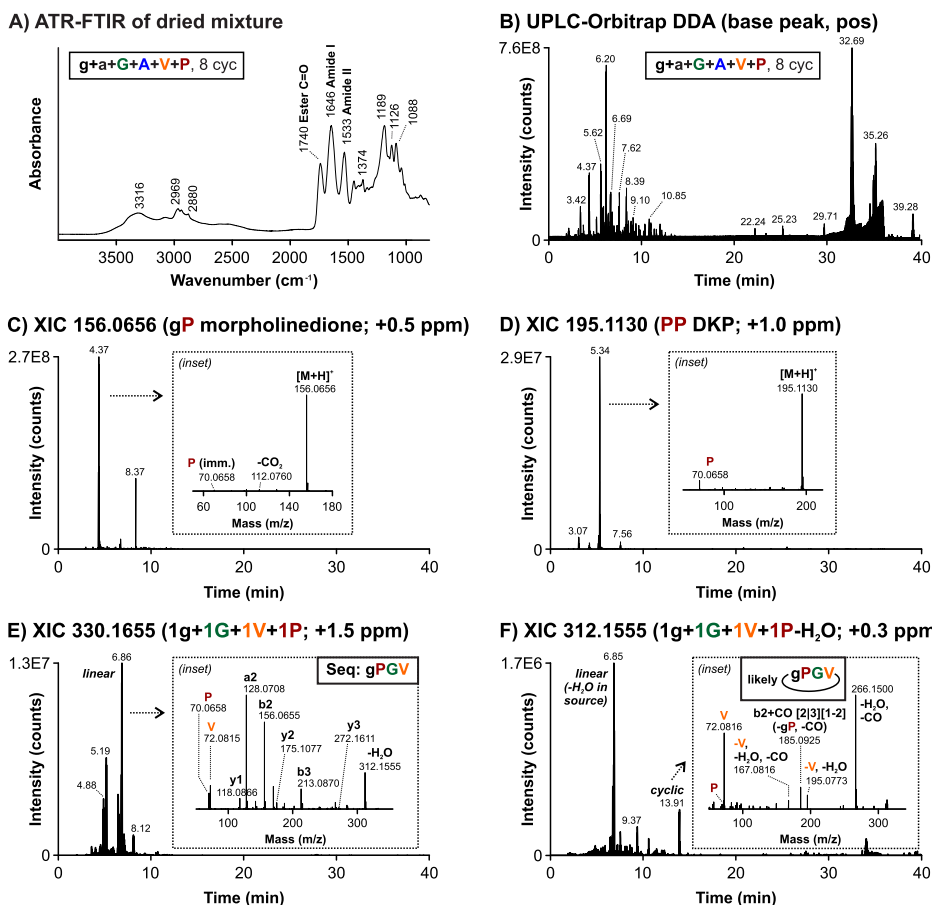


**Figure 6.** Analysis of a complex mixture by (A) FTIR and (B–F) DDA Orbitrap UPLC-MS/MS. (A) ATR-FTIR of 8-cycle sample shows ester, amide I, and amide II depsipeptide bands. (B) Base peak chromatogram of 8-cycle sample in positive ion mode. (C) XIC and in inset the MS/MS spectrum of gP morpholinedione,  $m/z$  156.0656. (D) XIC and in inset the MS/MS spectrum of Pro–Pro DPK,  $m/z$  195.1130. (E) XIC and in inset the MS/MS spectrum of linear gPGV,  $m/z$  330.1655. (F) XIC and in inset the MS/MS spectrum of cyclic 1g + 1G + 1V + 1P depsipeptide,  $m/z$  312.1555 and RT 13.91. The sequence was tentatively assigned as cyclo(gPGV). Signal at 6.85 min in (F) was assigned to  $\text{H}_2\text{O}$  loss from the linear oligomer in part (E).

Val suggests it preceded the glycolic acid ester linkage, likely the weakest on the backbone.<sup>77</sup> Third, the ester bond within the cyclic depsipeptide persisted after eight wet–dry cycles, suggesting that it may have been partially shielded from hydrolysis by the hydrophobic side chain of Val.

Another example of a linear oligomer and its cyclic counterpart (with  $n \geq 3$  residues) is provided in *Supporting Information* (Figures S14 and S15). It is possible that more cyclic species with 3+ residues were present but were missed by manual inspection or were not selected for MS/MS. Concerning the latter, DDA selects ions for fragmentation based on relative intensity, and cyclic sequences generally have low ionization efficiency as they lack ionizable termini.

## CONCLUSIONS

MALDI-TOF MS revealed that Pro incorporation into depsipeptides was more efficient than Gly, Ala, or Val when subjected to wet–dry cycling. However, Pro oligomers were somewhat shorter and were susceptible to mild in-source fragmentation ( $-\text{H}_2\text{O}$ ,  $-\text{CO}$  losses) during MALDI analysis. Targeted comparisons between Ala and Pro showed that Pro–Pro DPK, although a minor byproduct, slowly accumulated over time, whereas Ala–Ala DPK did not. We proposed that the greater propensity of Pro to adopt *cis* conformations may contribute to cyclization. In a more complex mixture analyzed

by high-resolution Orbitrap MS, the majority of products were again linear depsipeptides, yet small cyclic species were also present and often contained one or more Pro residues.

These findings naturally raise the follow-up questions. Could linear oligomers emerge abiotically with polyproline-like structure? Could plausible cyclic depsipeptides adopt rigid structures and/or demonstrate some type of catalytic activity? It is worth noting that numerous natural products in biology are, in fact, cyclic depsipeptides.<sup>78–83</sup> We seek to explore further the behavior of Pro in model prebiotic peptides and encourage others to do likewise.

## ASSOCIATED CONTENT

### Supporting Information

The Supporting Information is available free of charge at <https://pubs.acs.org/doi/10.1021/acsearthspacechem.0c00119>.

ESI-MS of a g+P binary mixture, LC-MS quantitation of DKPs, selected linear oligomers in complex mixture, more cyclic dimers with Pro in complex mixture, cyclic dimers without Pro in complex mixture, MALDI-FTICR MS of complex mixture, linear and cyclic tripeptide in complex mixture, and all oligomers detected by MALDI-TOF MS in binary mixtures (PDF)

## AUTHOR INFORMATION

### Corresponding Author

**Jay G. Forsythe** — *Department of Chemistry and Biochemistry, College of Charleston, Charleston, South Carolina 29424, United States; [orcid.org/0000-0003-1041-1113](https://orcid.org/0000-0003-1041-1113); Phone: (+1) 843-953-5052; Email: [forsythejg@cofc.edu](mailto:forsythejg@cofc.edu); Fax: (+1) 843-953-1404*

### Authors

**Jabbarius N. Ervin** — *Department of Chemistry and Biochemistry, College of Charleston, Charleston, South Carolina 29424, United States*

**Marcos Bouza** — *School of Chemistry and Biochemistry, Georgia Institute of Technology, Atlanta, Georgia 30332, United States*

**Facundo M. Fernández** — *School of Chemistry and Biochemistry, Georgia Institute of Technology, Atlanta, Georgia 30332, United States; [orcid.org/0000-0002-0302-2534](https://orcid.org/0000-0002-0302-2534)*

Complete contact information is available at:  
<https://pubs.acs.org/10.1021/acsearthspacechem.0c00119>

### Notes

The authors declare no competing financial interest.

## ACKNOWLEDGMENTS

This work was supported by NSF and NASA Astrobiology under the NSF Center for Chemical Evolution (CHE-1504217) and College of Charleston start-up funds to J.G.F. The authors thank the NSF MRI program for the linear ion trap at College of Charleston (CHE-1229559) and the 12T FTICR at Georgia Tech (CHE-1726528), as well as Clay Davis at NIST Hollings Marine Lab for access to and assistance with the Orbitrap QE Plus. We also thank Christopher Thompson (Bruker) for FTICR software assistance and the following persons for useful discussions and manuscript feedback: Martin C (Georgia Tech), Moran Frenkel-Pinter (Georgia Tech), Michael Giuliano (College of Charleston), Martha Grover (Georgia Tech), Nicholas Hud (Georgia Tech), Ram Krishnamurthy (The Scripps Research Institute), Luke Leman (The Scripps Research Institute), Charles Liotta (Georgia Tech), and Kelvin Smith (Georgia Tech).

## REFERENCES

- (1) Danger, G.; Plasson, R.; Pascal, R. Pathways for the formation and evolution of peptides in prebiotic environments. *Chem. Soc. Rev.* **2012**, *41*, 5416–5429.
- (2) Frenkel-Pinter, M.; Samanta, M.; Ashkenasy, G.; Leman, L. J. Prebiotic peptides: molecular hubs in the origin of life. *Chem. Rev.* **2020**, *120*, 4707.
- (3) Martin, R. B. Free energies and equilibria of peptide bond hydrolysis and formation. *Biopolymers* **1998**, *45*, 351–353.
- (4) Lahav, N.; White, D.; Chang, S. Peptide formation in the prebiotic era: thermal condensation of glycine in fluctuating clay environments. *Science* **1978**, *201*, 67–69.
- (5) Schwendiger, M. G.; Rode, B. M. Salt-induced formation of mixed peptides under possible prebiotic conditions. *Inorg. Chim. Acta* **1991**, *186*, 247–251.
- (6) Huber, C.; Wächtershäuser, G. Peptides by activation of amino acids with CO on (Ni,Fe)S surfaces: Implications for the origin of life. *Science* **1998**, *281*, 670–672.
- (7) Leman, L.; Orgel, L.; Ghadiri, M. R. Carbonyl sulfide-mediated prebiotic formation of peptides. *Science* **2004**, *306*, 283–286.
- (8) Griffith, E. C.; Vaida, V. In situ observation of peptide bond formation at the water-air interface. *Proc. Natl. Acad. Sci. U.S.A.* **2012**, *109*, 15697–15701.
- (9) Rodriguez-Garcia, M.; Surman, A. J.; Cooper, G. J. T.; Suarez-Marina, I.; Hosni, Z.; Lee, M. P.; Cronin, L. Formation of oligopeptides in high yield under simple programmable conditions. *Nat. Commun.* **2015**, *6*, 8385.
- (10) Canavelli, P.; Islam, S.; Pownar, M. W. Peptide ligation by chemoselective aminonitrile coupling in water. *Nature* **2019**, *571*, 546–549.
- (11) Forsythe, J. G.; Yu, S.-S.; Mamajanov, I.; Grover, M. A.; Krishnamurthy, R.; Fernández, F. M.; Hud, N. V. Ester-Mediated Amide Bond Formation Driven by Wet-Dry Cycles: A Possible Path to Polypeptides on the Prebiotic Earth. *Angew. Chem., Int. Ed.* **2015**, *54*, 9871–9875.
- (12) Yu, S.-S.; Krishnamurthy, R.; Fernandez, F. M.; Fernández, N. V.; Schork, F. J.; Grover, M. A. Kinetics of prebiotic depsipeptide formation from the ester-amide exchange reaction. *Phys. Chem. Chem. Phys.* **2016**, *18*, 28441–28450.
- (13) Yu, S.-S.; Solano, M. D.; Blanchard, M. K.; Soper-Hopper, M. T.; Krishnamurthy, R.; Fernández, F. M.; Hud, N. V.; Schork, F. J.; Grover, M. A. Elongation of model prebiotic proto-peptides by continuous monomer feeding. *Macromolecules* **2017**, *50*, 9286–9294.
- (14) Miller, S. L.; Urey, H. C. Organic Compound Synthesis on the Primitive Earth. *Science* **1959**, *130*, 245–251.
- (15) Peltzer, E. T.; Bada, J. L.  $\alpha$ -Hydroxycarboxylic acids in the Murchison meteorite. *Nature* **1978**, *272*, 443–444.
- (16) Huber, C.; Wächtershäuser, G.  $\alpha$ -Hydroxy and  $\alpha$ -Amino Acids Under Possible Hadean, Volcanic Origin-of-Life Conditions. *Science* **2006**, *314*, 630–632.
- (17) Parker, E. T.; Cleaves, H. J.; Bada, J. L.; Fernández, F. M. Quantitation of  $\alpha$ -hydroxy acids in complex prebiotic mixtures via liquid chromatography/tandem mass spectrometry. *Rapid Commun. Mass Spectrom.* **2016**, *30*, 2043–2051.
- (18) Kua, J.; Sweet, L. M. Preliminary oligomerization in a glycolic acid-glycine mixture: a free energy map. *J. Phys. Chem. A* **2016**, *120*, 7577–7588.
- (19) Mamajanov, I.; MacDonald, P. J.; Ying, J.; Duncanson, D. M.; Dowdy, G. R.; Walker, C. A.; Engelhart, A. E.; Fernández, F. M.; Grover, M. A.; Hud, N. V.; Schork, F. J. Ester formation and hydrolysis during wet-dry cycles: generation of far-from-equilibrium polymers in a model prebiotic reaction. *Macromolecules* **2014**, *47*, 1334–1343.
- (20) Davila, A. F.; Dupont, L. G.; Melchiorri, R.; Jänen, J.; Valea, S.; de los Rios, A.; Fairén, A. G.; Möhlmann, D.; McKay, C. P.; Ascaso, C.; Wierzchowski, J. Hygroscopic salts and the potential for life on Mars. *Astrobiology* **2010**, *10*, 617–628.
- (21) Chatterjee, S. A symbiotic view of the origin of life at hydrothermal impact crater-lakes. *Phys. Chem. Chem. Phys.* **2016**, *18*, 20033–20046.
- (22) Martín-Torres, F. J.; Zorzano, M.-P.; Valentín-Serrano, P.; Harri, A.-M.; Genzer, M.; Kemppinen, O.; Rivera-Valentin, E. G.; Jun, I.; Wray, J.; Bo Madsen, M.; Goetz, W.; McEwen, A. S.; Hardgrove, C.; Renno, N.; Chevrier, V. F.; Mischna, M.; Navarro-González, R.; Martínez-Frías, J.; Conrad, P.; McConnochie, T.; Cockell, C.; Berger, G.; Vasavada, A. R.; Sumner, D.; Vaniman, D. Transient liquid water and water activity at Gale crater on Mars. *Nat. Geosci.* **2015**, *8*, 357–361.
- (23) Ojha, L.; Wilhelm, M. B.; Murchie, S. L.; McEwen, A. S.; Wray, J. J.; Hanley, J.; Massé, M.; Chojnacki, M. Spectral evidence for hydrated salts in recurring slope lineae on Mars. *Nat. Geosci.* **2015**, *8*, 829–832.
- (24) Deamer, D.; Damer, B.; Kompanichenko, V. Hydrothermal Chemistry and the Origin of Cellular Life. *Astrobiology*, **2019** 1915231537
- (25) Campbell, T. D.; Febrian, R.; McCarthy, J. T.; Kleinschmidt, H. E.; Forsythe, J. G.; Bracher, P. J. Prebiotic condensation through wet-dry cycling regulated by deliquescence. *Nat. Commun.* **2019**, *10*, 4508.

(26) Zaia, D. A. M.; Zaia, C. T. B. V.; De Santana, H. Which amino acids should be used in prebiotic chemistry studies? *Orig. Life Evol. Biosph.* **2008**, *38*, 469–488.

(27) Trifonov, E. N. Consensus temporal order of amino acids and evolution of the triplet code. *Gene* **2000**, *261*, 139–151.

(28) Piszkiewicz, D.; Landon, M.; Smith, E. L. Anomalous cleavage of aspartyl-proline peptide bonds during amino acid sequence determinations. *Biochem. Biophys. Res. Commun.* **1970**, *40*, 1173–1178.

(29) Levitt, M. Effect of proline residues on protein folding. *J. Mol. Biol.* **1981**, *145*, 251–263.

(30) Brandts, J. F.; Halvorson, H. R.; Brennan, M. Consideration of the possibility that the slow step in protein denaturation reactions is due to cis-trans isomerism of proline residues. *Biochemistry* **1975**, *14*, 4953–4963.

(31) Wedemeyer, W. J.; Welker, E.; Scheraga, H. A. Proline Cis–Trans Isomerization and Protein Folding. *Biochemistry* **2002**, *41*, 14637–14644.

(32) Pierson, N. A.; Chen, L.; Russell, D. H.; Clemmer, D. E. Cis–TransIsomerizations of Proline Residues Are Key to Bradykinin Conformations. *J. Am. Chem. Soc.* **2013**, *135*, 3186–3192.

(33) Macarthur, M. W.; Thornton, J. M. Influence of proline residues on protein conformation. *J. Mol. Biol.* **1991**, *218*, 397–412.

(34) Barlow, D. J.; Thornton, J. M. Helix geometry in proteins. *J. Mol. Biol.* **1988**, *201*, 601–619.

(35) Cowan, P. M.; McGavin, S. Structure of poly-L-proline. *Nature* **1955**, *176*, 501–503.

(36) Steinberg, I. Z.; Harrington, W. F.; Berger, A.; Sela, M.; Katchalski, E. The configurational changes of poly-L-proline in solution. *J. Am. Chem. Soc.* **1960**, *82*, 5263–5279.

(37) Adzhubei, A. A.; Sternberg, M. J. E. Left-handed polyproline II helices commonly occur in globular proteins. *J. Mol. Biol.* **1993**, *229*, 472–493.

(38) Counterman, A. E.; Clemmer, D. E. Anhydrous polyproline helices and globules. *J. Phys. Chem. B* **2004**, *108*, 4885–4898.

(39) Pavlov, M. Y.; Watts, R. E.; Tan, Z.; Cornish, V. W.; Ehrenberg, M.; Forster, A. C. Slow peptide bond formation by proline and other N-alkylamino acids in translation. *Proc. Natl. Acad. Sci. U.S.A.* **2009**, *106*, 50–54.

(40) List, B.; Lerner, R. A.; Barbas, C. F. Proline-catalyzed direct asymmetric aldol reactions. *J. Am. Chem. Soc.* **2000**, *122*, 2395–2396.

(41) List, B. Proline-catalyzed asymmetric reactions. *Tetrahedron* **2002**, *58*, 5573–5590.

(42) Mathew, S. P.; Iwamura, H.; Blackmond, D. G. Amplification of enantiomeric excess in a proline-mediated reaction. *Angew. Chem., Int. Ed.* **2004**, *43*, 3317–3321.

(43) Kumaragurubaran, N.; Juhl, K.; Zhuang, W.; Bøgevig, A.; Jørgensen, K. A. Direct-Proline-Catalyzed Asymmetric  $\alpha$ -Amination of Ketones. *J. Am. Chem. Soc.* **2002**, *124*, 6254–6255.

(44) Breslow, R.; Cheng, Z.-L. L-amino acids catalyze the formation of an excess of D-glyceraldehyde, and thus of other D sugars, under credible prebiotic conditions. *Proc. Natl. Acad. Sci. U.S.A.* **2010**, *107*, 5723–5725.

(45) Hein, J. E.; Tse, E.; Blackmond, D. G. A route to enantiopure RNA precursors from nearly racemic starting materials. *Nat. Chem.* **2011**, *3*, 704–706.

(46) Blackmond, D. G. The origin of biological homochirality. *CSH Perspect. Biol.* **2010**, *2*, a002147.

(47) Hein, J. E.; Blackmond, D. G. On the origin of single chirality of amino acids and sugars in biogenesis. *Acc. Chem. Res.* **2012**, *45*, 2045–2054.

(48) Brotzel, F.; Chu, Y. C.; Mayr, H. Nucleophilicities of primary and secondary amines in water. *J. Org. Chem.* **2007**, *72*, 3679–3688.

(49) Deber, C. M.; Madison, V.; Blout, E. R. Why cyclic peptides? Complementary approaches to conformations. *Acc. Chem. Res.* **1976**, *9*, 106–113.

(50) English, S. L.; Forsythe, J. G. Matrix-assisted laser desorption/ionization time-of-flight mass spectrometry of model prebiotic peptides: optimization of sample preparation. *Rapid Commun. Mass Spectrom.* **2018**, *32*, 1507–1513.

(51) Ma, B.; Zhang, K.; Hendrie, C.; Liang, C.; Li, M.; Doherty-Kirby, A.; Lajoie, G. PEAKS: powerful software for peptide de novo sequencing by tandem mass spectrometry. *Rapid Commun. Mass Spectrom.* **2003**, *17*, 2337–2342.

(52) Niedermeyer, T. H. J.; Strohalm, M. mMass as a software tool for the annotation of cyclic peptide tandem mass spectra. *PLOS One* **2012**, *7*, No. e44913.

(53) Stephenson, R. C.; Clarke, S. Succinimide formation from aspartyl and asparaginyl peptides as a model for the spontaneous degradation of proteins. *J. Biol. Chem.* **1989**, *264*, 6164–6170.

(54) González, L. J.; Shimizu, T.; Satomi, Y.; Betancourt, L.; Besada, V.; Padrón, G.; Orlando, R.; Shirasawa, T.; Shimonishi, Y.; Takao, T. Differentiating alpha- and beta-aspartic acids by electrospray ionization and low-energy tandem mass spectrometry. *Rapid Commun. Mass Spectrom.* **2000**, *14*, 2092–2102.

(55) Hurtado, P. P.; O'Connor, P. B. Differentiation of isomeric amino acid residues in proteins and peptides using mass spectrometry. *Mass Spectrom. Rev.* **2012**, *31*, 609–625.

(56) Frenkel-Pinter, M.; Haynes, J. W.; C, M.; Petrov, A. S.; Burcar, B. T.; Krishnamurthy, R.; Hud, N. V.; Leman, L. J.; Williams, L. D. Selective incorporation of proteinaceous over nonproteinaceous cationic amino acids in model prebiotic oligomerization reactions. *Proc. Natl. Acad. Sci. U.S.A.* **2019**, *116*, 16338–16346.

(57) Deechongkit, S.; Dawson, P. E.; Kelly, J. W. Toward Assessing the Position-Dependent Contributions of Backbone Hydrogen Bonding to  $\beta$ -Sheet Folding Thermodynamics Employing Amide-to-Ester Perturbations. *J. Am. Chem. Soc.* **2004**, *126*, 16762–16771.

(58) Nielsen, M. W. F. MALDI time-of-flight mass spectrometry of synthetic polymers. *Mass Spectrom. Rev.* **1999**, *18*, 309–344.

(59) Kricheldorf, H. R. Cyclic polymers: synthetic strategies and physical properties. *J. Polym. Sci., Part A: Polym. Chem.* **2010**, *48*, 251–284.

(60) Asakawa, D.; Smargiasso, N.; Quinton, L.; de Pauw, E. Influences of proline and cysteine residues on fragment yield in matrix-assisted laser desorption/ionization in-source decay mass spectrometry. *J. Am. Soc. Mass Spectrom.* **2014**, *25*, 1040–1048.

(61) Kvenvolden, K.; Lawless, J.; Pering, K.; Peterson, E.; Flores, J.; Ponnamperuma, C.; Kaplan, I. R.; Moore, C. Evidence for extraterrestrial amino-acids and hydrocarbons in the Murchison meteorite. *Nature* **1970**, *228*, 923–926.

(62) Doran, D.; Abul-Haija, Y. M.; Cronin, L. Emergence of function and selection from recursively programmed polymerisation reactions in mineral environments. *Angew. Chem., Int. Ed.* **2019**, *58*, 11253–11256.

(63) Ying, J.; Lin, R. C.; Xu, P. X.; Wu, Y. L.; Liu, Y.; Zhao, Y. F. Prebiotic formation of cyclic dipeptides under potentially early earth conditions. *Sci. Rep.* **2018**, *8*, 936.

(64) Sibilska, I.; Chen, B.; Li, L.; Yin, J. Effects of trimetaphosphate on abiotic formation and hydrolysis of peptides. *Life (Basel)* **2017**, *7*, 50.

(65) Fischer, P. M. Diketopiperazines in peptide and combinatorial chemistry. *J. Pept. Sci.* **2003**, *9*, 9–35.

(66) Orgel, L. E. The origin of polynucleotide-directed protein synthesis. *J. Mol. Evol.* **1989**, *29*, 465–474.

(67) Hayakawa, S.; Hashimoto, M.; Matsubara, H.; Tureček, F. Dissecting the Proline Effect: Dissociations of Proline Radicals Formed by Electron Transfer to Protonated Pro-Gly and Gly-Pro Dipeptides in the Gas Phase. *J. Am. Chem. Soc.* **2007**, *129*, 7936–7949.

(68) Fuller, D. R.; Conant, C. R.; El-Baba, T. J.; Brown, C. J.; Woodall, D. W.; Russell, D. H.; Clemmer, D. E. Conformationally regulated peptide bond cleavage in bradykinin. *J. Am. Chem. Soc.* **2018**, *140*, 9357–9360.

(69) Conant, C. R.; Fuller, D. R.; El-Baba, T. J.; Zhang, Z.; Russell, D. H.; Clemmer, D. E. Substance P in solution: trans-to-cis configurational changes of penultimate prolines initiate non-

enzymatic peptide bond cleavages. *J. Am. Soc. Mass Spectrom.* **2019**, *30*, 919–931.

(70) Parker, E. T.; Zhou, M.; Burton, A. S.; Glavin, D. P.; Dworkin, J. P.; Krishnamurthy, R.; Fernández, F. M.; Bada, J. L. A plausible simultaneous synthesis of amino acids and simple peptides on the primordial earth. *Angew. Chem., Int. Ed.* **2014**, *53*, 8132–8136.

(71) Toniolo, C.; Crisma, M.; Formaggio, F.; Peggion, C. Control of peptide conformation by the Thorpe-Ingold Effect. *Biopolymers* **2001**, *60*, 396–419.

(72) Horne, W. S.; Price, J. L.; Gellman, S. H. Interplay among side chain sequence, backbone composition, and residue rigidification in polypeptide folding and assembly. *Proc. Natl. Acad. Sci. U.S.A.* **2008**, *105*, 9151–9156.

(73) Reinert, Z. E.; Horne, W. S. Folding thermodynamics of protein-like oligomers with heterogeneous backbones. *Chem. Sci.* **2014**, *5*, 3325–3330.

(74) Ngoka, L. C. M.; Gross, M. L. A nomenclature system for labeling cyclic peptide fragments. *J. Am. Soc. Mass Spectrom.* **1999**, *10*, 360–363.

(75) Harrison, A. G. Fragmentation Reactions of b5 and a5 Ions Containing Proline-The Structures of a5 Ions. *J. Am. Soc. Mass Spectrom.* **2012**, *23*, 594–601.

(76) Liu, W.-T.; Ng, J.; Meluzzi, D.; Bandeira, N.; Gutierrez, M.; Simmons, T. L.; Schultz, A. W.; Linington, R. G.; Moore, B. S.; Gerwick, W. H.; Pevzner, P. A.; Dorrestein, P. C. Interpretation of tandem mass spectra obtained from cyclic nonribosomal peptides. *Anal. Chem.* **2009**, *81*, 4200–4209.

(77) Banerjee, R.; Sudarsal, S.; Ranganayaki, R. S.; Raghothama, S. Effect of ester chemical structure and peptide bond conformation in fragmentation pathways of differently metal cationized cyclodepsipeptides. *Org. Biomol. Chem.* **2011**, *9*, 6234–6245.

(78) Pinkerton, M.; Steinrauf, L. K.; Dawkins, P. The molecular structure and some transport properties of valinomycin. *Biochem. Biophys. Res. Commun.* **1969**, *35*, 512–518.

(79) Fernández, R.; Rodríguez, J.; Quiñoá, E.; Riguera, R.; Muñoz, L.; Fernández-Suárez, M.; Debitus, C. Onchidin B: A New Cyclodepsipeptide from the Mollusc *Onchidium* sp. *J. Am. Chem. Soc.* **1996**, *118*, 11635–11643.

(80) Suzuki, Y.; Ojika, M.; Sakagami, Y.; Kaida, K.; Fudou, R.; Kameyama, T. New Cyclic Depsipeptide Antibiotics, Clavariopsins A and B, Produced by an Aquatic Hyphomycetes, *Clavariopsis aquatica*. *J. Antibiot.* **2001**, *54*, 22–28.

(81) Hamada, Y.; Shioiri, T. Recent progress of the synthetic studies of biologically active marine cyclic peptides and depsipeptides. *Chem. Rev.* **2005**, *105*, 4441–4482.

(82) Thakur, S. S.; Ranganayaki, R. S.; Gupta, K.; Balaram, P. Identification of  $\alpha$ - and  $\beta$ -hydroxy acid containing cyclodepsipeptides in natural peptide mixtures using negative ion mass spectrometry. *J. Am. Soc. Mass Spectrom.* **2009**, *20*, 2221–2228.

(83) Fang, W.-Y.; Dahiya, R.; Qin, H. L.; Mourya, R.; Maharaj, S. Natural proline-rich cyclopolyptides from marine organisms: chemistry, synthetic methodologies and biological status. *Mar. Drugs* **2016**, *14*, 194.